JOURNAL OF MATERIALS SCIENCE 30 (1995) 4014–4018

Modelling of multilayer films using spectroscopic ellipsometry

K. CHATTOPADHYAY, J. AUBEL, S. SUNDARAM
Department of Physics, University of South Florida, Tampa, FL 33620, USA

A systematic investigation of the ellipsometric parameters of MBE-grown heterostructures of $In_xGa_{1-x}As$ on GaAs substrate has been completed. The index of refraction n, and extinction coefficient, k, values of the above heterostructure in the wavelength range 500–800 nm, are presented, a region of interest in many applications. A model has been proposed for the multilayered structures, through which the thickness of the oxide layer can be determined and the observed optical characteristics of these heterostructures explained. The validity of the model was established by the excellent agreement between the measured and calculated values of the ellipsometric parameters ψ and Δ.

1. Introduction

In recent years there has been an intense research effort on semiconductor heterojunctions. An increasingly important flexibility in the design and fabrication of many types of high-performance electronic devices is obtained by the use of heterostructure materials. Much of the work on such structures was performed with lattice-matched materials, but scientific and industrial interest has extended to the lattice-mismatched materials as well. Compound semiconductors consisting of elements from the groups III and V of the periodic table and their alloys have attracted much interest from the viewpoint of applications to high-speed optoelectronic devices. More specifically, the epitaxial layers of these ternary or quaternary compounds on binary substrates are of interest for such applications. InGaAs quantum wells are particularly attractive because the InGaAs layer can serve as the transmission medium which is transparent to the photon energy near the InGaAs band gap. Our interest was particularly on InGaAs grown on GaAs substrate. This formed a strained layer because there is a lattice mismatch. So we wanted to study the effect of these strains on the dielectric constants.

Ellipsometry has been shown to be a viable technique for measuring the layer thickness [1, 2] and interfacial properties of GaAs–$In_xGa_{1-x}As$ multiple layer structures. Thus in the present study, the technique of variable angle spectroscopic ellipsometry (VASE) was used for the purpose of investigating the optical properties of GaAs–$In_xGa_{1-x}As$ heterostructures. It is also shown that a combination of variable angles of incidence and variable wavelength capabilities will achieve the highest possible sensitivity and accuracy in measurements of multiple layer structures. Our main objective was more towards the development of a mathematical model to study the heterostructures in more detail. The experimental measurements gave the properties of the whole composite structure and did not take into account the different layers and also the oxide thickness. So in this study we have proposed a multilayer model which helps to determine the oxide layer thickness and explain the observed optical characteristics of these heterostructures.

2. Experimental procedure

As shown by a number of authors and previous investigations, one of the most effective optical probes for the study of films and bulk materials in a truly non-destructive way over a given wavelength range is spectroscopic polarization modulation ellipsometry (SPME) [3–6]. In this experiment, light emerging from the monochromator is polarized at 45° with respect to the axes of a piezo-electric birefringence modulator. All angles are measured from zero with respect to the vertical (+ s) set as zero. Positive angles are measured as a counter clockwise rotation from the + s axis as the observer faces the source. After reflection at the sample surface, the polarization modulation is converted to intensity modulation by an analyser and detected by a silicon diode detector. In the following ellipsometer experiments [7] the spectra were measured in the five configurations necessary to acquire the SPME data. A lock-in phase-sensitive detector was used to obtain the intensities corresponding to the first- and second-order frequency harmonics I_ω and $I_{2\omega}$, where ω is the frequency. The frequency-independent term I_0 was measured with a d.c. voltmeter. The amplitude of the modulation was set such that the zero-order Bessel function, $J_0(A)$, is zero throughout a scan. This condition exists as long as the amplitude of the modulator corresponds to a retardation of 137.5°. Under the described conditions, the first- and second-order frequency harmonics are given by

$$R_\omega = \frac{I_\omega}{I_o} = \frac{-2|\rho|\sin\Delta[2J_1(A_m)]}{1+|\rho|^2} \quad (1)$$

0022–2461

$$R_{2\omega} = \frac{I_{2\omega}}{I_0}$$

$$= \frac{(1 - |\rho|^2)}{(1 + |\rho|^2)} 2J_2(A_m) \quad (2)$$

for the 50 and 100 kHz signal, respectively. In the above equations $\rho = R_p/R_s = \tan\psi \exp(i\Delta)$ and R_p and R_s are the complex reflectances parallel and perpendicular to the incident beam and A_m is the modulation amplitude. The standard ellipsometric parameters, ψ and Δ, are defined by $\tan\psi = r_p/r_s$ = the ratio of the Fresnel coefficients, and $\Delta = \delta_p - \delta_s$ = the phase shift difference. Among the five configurations mentioned earlier, there are two which are referred to as calibration configurations because they determine the non-zero-order Bessel functions. These give

$$R_{2\omega}^{cal} = \frac{I_{2\omega}^{cal}}{I_0^{cal}}$$

$$= 2J_2(A_m) \quad (3)$$

$$R_{\omega}^{cal} = \frac{I_{\omega}^{cal}}{I_0^{cal}}$$

$$= 2J_1(A_m) \quad (4)$$

From these measurements N, S, and C values are computed using the following equations

$$N = \frac{R_{2\omega}}{R_{2\omega}^{cal}} \quad (5)$$

$$S = \frac{R_{\omega}}{R_{\omega}^{cal}} \quad (6)$$

$$C = \frac{R_{2\omega}}{R_{2\omega}^{cal}} \quad (7)$$

Theoretically N, S, and C should be components of a unit vector, so

$$\beta^2 = N^2 + S^2 + C^2 - 1 \quad (8)$$

gives an estimate of the accuracy of experimental alignments as well as the measurements. Special care was taken to ensure the accuracy of experimental measurements and the β value was kept less than 1.5% for most of the present measurements. These measurements were reproducible to a high degree and thus our data were fairly consistent.

InGaAs samples with two different mole fractions of indium i.e. 10% and 20%, and three different thicknesses of the InGaAs layer, were used. The samples of InGaAs used in this study were provided by Dr H. Morkoc and Dr D. Huang, University of Illinois, Urbana, IL. The epitaxial layers of these samples were 2–4.5 μm thick and grown by the molecular beam epitaxial technique (MBE) using elemental indium, gallum and arsenic sources. These layers were grown on undoped semi-insulating GaAs substrates following the deposition of a 0.5–1.0 μm thick MBE GaAs buffer layer. The InGaAs layers were grown under arsenic-stabilized conditions and the composition was varied by adjusting the incident indium flux while maintaining a fixed gallium flux. The InGaAs is capped by a 30 nm thick GaAs layer.

3. Results

With the experimental equipment described earlier by Bermudez and Ritz [7], the N, S and C values were measured from five different configurations. In terms of the ellipsometric parameters ψ and Δ, the quantities N, S and C are defined as

$$N = \cos(2\psi) \quad (9)$$

$$S = \sin(2\psi)\sin(\Delta) \quad (10)$$

$$C = \sin(2\psi)\cos(\Delta) \quad (11)$$

The measurements were done for four different angles of incidence, ϕ. The dielectric constants, ε_1 and ε_2, were calculated from the measured ψ and Δ values using the following equations [7]

$$\varepsilon_1 = \sin^2\phi \tan^2\phi \frac{(N^2 - S^2)}{(1 + C)^2} + \sin^2\phi \quad (12)$$

$$\varepsilon_2 = 2\sin^2\phi \tan^2\phi \frac{NS}{(1 + C)^2} \quad (13)$$

As mentioned in the previous section, our sample was a multilayer heterostructure and these measured optical constants were characteristic for the whole composite structure. As noted earlier, one of our main objectives was to propose a valid model which would enable us to determine the optical characteristics of InGaAs and also the thickness of the oxide layer.

Now the thicknesses, t_1 and t_2, of InGaAs and GaAs, respectively, were known. The oxide thickness, d_{ox}, was not known and the help of the model was needed to calculate this quantity. Thus, in our samples, we actually consider four interface layers which are (a) I_{01} (air–oxide), (b) I_{12} (oxide–GaAs), (c) I_{23} (GaAs–InGaAs) and (d) I_{34} (InGaAs–GaAs). The three different layers are (a) L_1 (oxide), (b) L_2 (GaAs) and (c) L_3 (InGaAs). We developed a program (using the MATHCAD computer program), which calculated the stratified structure scattering matrix, S_n, (product of layer and interface matrices), for both linear polarizations parallel (p) and perpendicular (s) to the plane of incidence. The ratios of these scattering matrices for the p and s polarizations give us the complex reflection coefficients R_p and R_s. The MATHCAD program does all the rigorous calculations of the Jones interface and layer matrices [8] to determine ψ_c and Δ_c, using the following equations

$$\psi_c = \tan^{-1}|\rho_c| \quad (14)$$

$$\Delta_c = \arg[\rho_c] \quad (15)$$

where $\rho_c = R_p/R_s$, $|\rho_c|$ and $\arg|\rho_c|$ are the absolute value and the argument (angle) of the complex function ρ_c. The MATHCAD program used here also calculated the ψ_m and Δ_m of the composite structure from the measured values of N, S, and C using Equations 10–12. The index of refraction, n, and extinction coefficient, k, values for the GaAs were taken from the literature [9]. The data used to model the native oxide

TABLE I Comparison of n and k values of $In_xGa_{1-x}As$ for $x = 0.1$, 0.2 and 0.53. The value for $x = 0.53$ has been taken from the literature.

Wavelength	$d_{ox} = 3.9$ nm, $G = 3.65 \times 10^{-3}$ $x = 0.1$		$d_{ox} = 4.8$ nm, $G = 3.65 \times 10^{-3}$ $x = 0.2$		$x = 0.53$	
λ(nm)	n	k	n	k	n	k
500	4.58	0.57	4.68	0.37	4.59	1.19
540	4.33	0.385	4.39	0.36	4.32	0.74
560	4.23	0.38	4.29	0.355	4.23	0.64
590	4.13	0.375	4.20	0.35	4.10	0.52
620	4.07	0.37	4.13	0.34	4.02	0.48
650	4.02	0.365	4.05	0.33	3.95	0.43
690	3.93	0.36	3.98	0.32	3.88	0.37
730	3.87	0.35	3.93	0.31	3.82	0.30

layer and its relation to the heterostructure values were also taken from the literature [10]. As mentioned in the previous study, $n_{ox} = 1.9$ was assumed to be constant for different wavelengths, because it has negligible effect on the n_f and k_f values of InGaAs and on the thickness of the oxide layer. Attempts were also made to vary the value of n_{ox} with wavelength, but calculations indicated that it has negligible effect on the thickness of the oxide layer. Just for the sake of a reference point, the n and k values of $In_xGa_{1-x}As$ ($x = 0.53$) from the literature [11] are included. The value of oxide thickness, d_{ox}, and n, k of InGaAs were fitted by minimizing the sum [11, 12]

$$G = \Sigma[(\Delta_{c_j} - \Delta_{m_j})^2 + (\psi_{c_j} - \psi_{m_j})^2] \quad (16)$$

where j denotes wavelength. In this equation "m" denotes the measured values and "c" denotes the calculated values of ψ and Δ. Different sets of n and k were tried for InGaAs as well as the oxide layer thickness to match the ψ and Δ curves obtained from measured and calculated values.

4. Discussion

In Table I, the values of n and k for samples with $x = 0.1$ and $x = 0.2$ are summarized. In the same table, the thicknesses of the oxide layers are given as obtained from our model and the G values are also indicated. Fig. 1a and b show the relations of ψ versus λ and Δ versus λ, respectively. Although we have investigated three samples with InGaAs thickness of 10, 20, and 30 nm, respectively, for $x = 0.1$ and 0.2, in the above figures the results for only one typical sample are shown. As expected, the curve with calculated ψ_c and Δ_c values did not match the curve with measured values of ψ_m and Δ_m. This is the case because we used the n and k values of InGaAs of 0.53 mole fraction, whereas the samples in our experiments had 10% and 20% mole fractions of indium, respectively. Another reason for the curves not being in agreement is the thickness of the native oxide layer. The correct d_{ox}, n and k of InGaAs were fitted by minimizing the sum, as mentioned earlier (Equation 16). It must be noted that in our present studies, these sums are of the order of 10^{-3}, thus supporting the validity of the results here (see Table I).

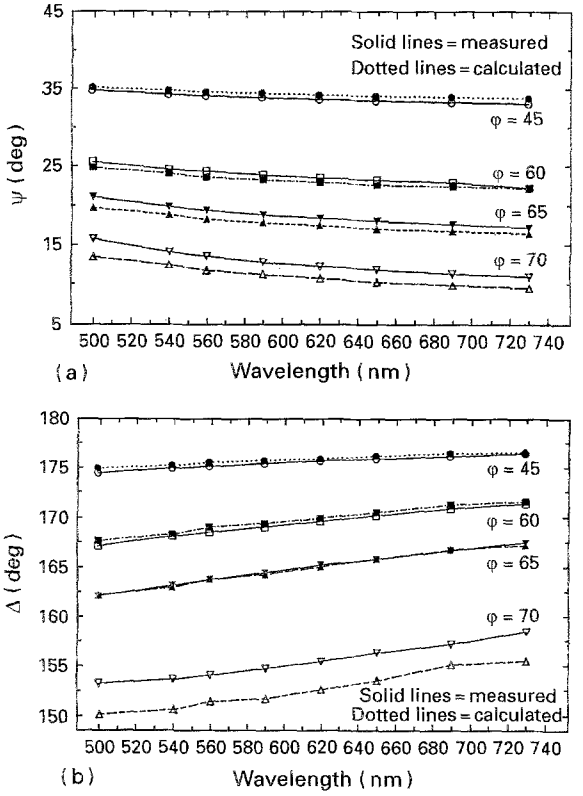

Figure 1 Plots of measured and calculated Ψ and (b) measured and calculated Δ, of InGaAs and wavelength.

It is clear from Fig. 1 that for angles of incidence 45°, 60° and 65°, the curves fit very well for both ψ and Δ. In the case of 70° angle of incidence, some discrepancy is observed because the curves do not match very well. We believe this has something to do with the sensitivity of ψ and Δ with angles of incidence. It had been shown in a previous investigation by Snyder *et al.* [13] on the sensitivity of ellipsometric parameters, that ψ and Δ are both very sensitive near 70°–75° angle of incidence and our results are in agreement with this observation. Further, it was shown that Δ is more sensitive than ψ for the same angle of incidence. Our results and the graphs confirmed both these observations because we could not match the ψ and Δ curves at 70° angle of incidence. Furthermore, at this particular angle, Δ_m and Δ_c are further apart compared to ψ_m and ψ_c. The n and k values of InGaAs for the two different mole fractions are given in Table I.

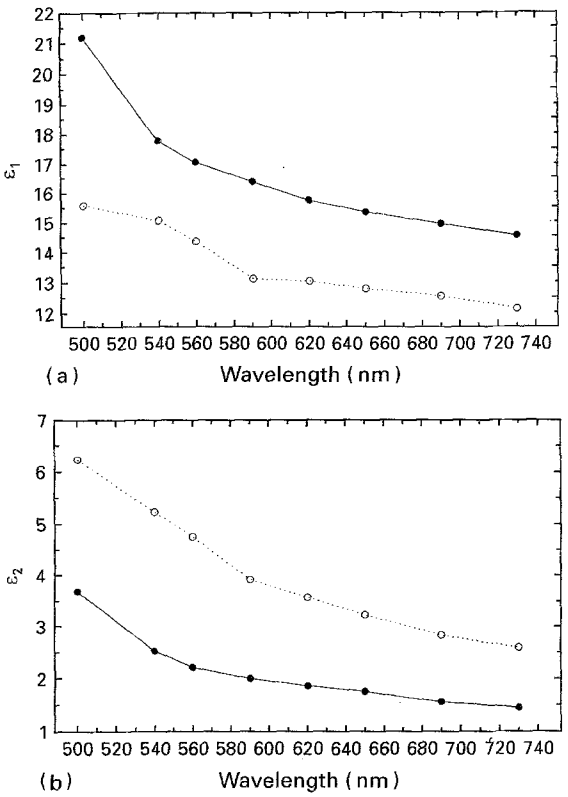

Figure 2 Correlations of (a) ε_1, and (b) ε_2, with wavelength for (--○--) the composite structure and (—●—) InGaAs.

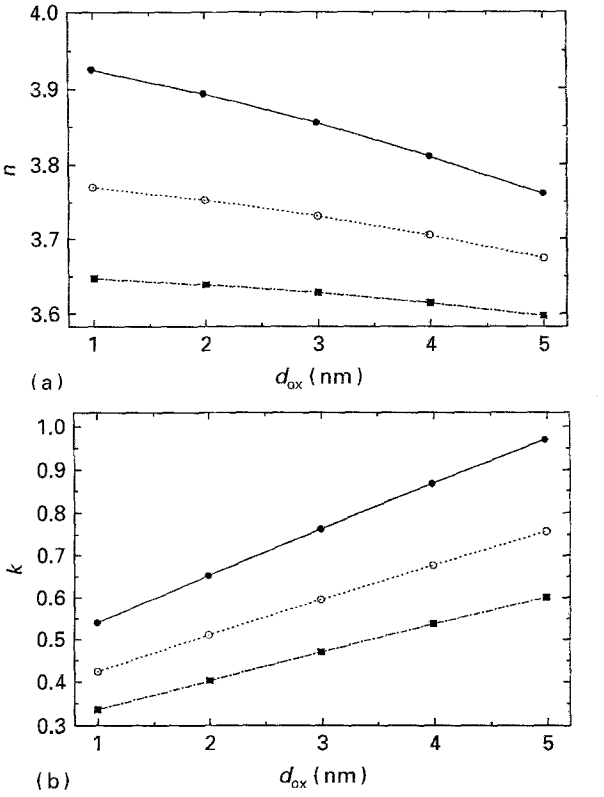

Figure 3 Correlations of (a) refractive index, n, and (b) extinction coefficient, k, with the oxide thickness, d_{ox}, for specific wavelengths: (●) 540 nm, (○) 620 nm, (■) 730 nm.

We also calculated the dielectric constants, ε_1 and ε_2 from the measured N, S and C values. But again these are the values of the composite structure and not of InGaAs only. Therefore, again our model was used to evaluate the real ε_1 and ε_2 values of InGaAs. These values for the composite structure and InGaAs values of ε_1 and ε_2 are shown in Fig. 2. It was very clear from these observations that the presence of the oxide layer has a significant effect on the ε_1 and ε_2 values. As parts of this study, attempts were made to find the effect of oxide layer of different thickness on the values of n and k. The n value decreases with increasing oxide thickness. The k value increases with the oxide thickness which is as expected. Actually, k measures the absorption coefficient of the material, and hence the larger the oxide thickness, the higher will be the absorption. This was confirmed by our observation and the resulting graph, as shown in Fig. 3, where the variations of n and k with oxide thickness are shown for three typical wavelengths of the probe light.

5. Conclusion

A systematic investigation of the ellipsometric parameters of the heterostructures of $In_xGa_{1-x}As$ ($x = 0.1$ and 0.2) grown by MBE technique on GaAs substrate has been completed. The values of the index of refraction, n, and the extinction coefficient, k, have been obtained for a range of wavelengths extending from 500–800 nm. The effects of the oxide layer on top surfaces of the above heterostructures have been studied in the same wavelength range. Most importantly, models have been developed to explain the observed optical characteristics of the heterostructures and the validity of the model established based on the excellent agreement between the measured and calculated values of the ellipsometric parameters, ψ and Δ. Also, the dielectric functions, ε_1 and ε_2, of the composite structures and hence the ε_1 and ε_2 of InGaAs, have been obtained for the wavelength range 500–800 nm. Finally, the variation of the index of refraction and the extinction coefficient with changes in the thickness of the oxide layer have been investigated for the same wavelength range.

In conclusion, the most significant result is that it has been shown that it is possible to establish satisfactory models for the multilayered heterostructures of electronic materials using the experimentally measured values of the ellipsometric parameters. Spectroscopic ellipsometry is thus a powerful tool for the optical characterization of the heterostructures and the nature of the interfaces. The method for deriving models for the multilayers should be extended to other investigations and thus generate a data base on heterostructures of these ternaries which are so useful in device applications.

References

1. S. M. SZE, "Physics of semiconductor devices" (Wiley, New York, 1981).
2. M. ERMAN, J. B. THEETEN, N. VODJDANI and Y. DEMAY, *J. Vac. Sci. Technol.* **B1** (1983) 328.
3. S. N. JASPERSON and S. E. SCHNATTERLY, *Rev. Sci. Instrum.* **40** (1969) 761.
4. J. I. TREU, A. B. CALLENDER and S. E. SCHNATTERLY, *ibid.* **37** (1973) 793.

5. S. N. JASPERSON, D. K. BURGE and R. C. O'HANDLEY, *Surf. Sci.* **45** (1974) 19.
6. J. I. TREU, *Rev. Sci. Instrum.* **45** (1974) 1467.
7. V. M. BERMUDEZ and V. H. RITZ, *Appl. Opt.* **17** (1978) 542.
8. R. M. A. AZZAM and N. M. BASHARA, "Ellipsometry and polarized light", (North-Holland, New York, 1977) p. 153.
9. D. E. ASPENS and A. A. STUDNA, *Phys. Rev. B* **27** (1983) 985.
10. M. BURKHARD, H. W. DINGES and E. KUPHAL, *J. Appl. Phys.* **53** (1982) 655.
11. H. W. DINGES, H. BURKHARD, R. LOSCH, H. NICKEL and W. SCLAPP, *Appl. Surf. Sci.* **54** (1992) 477.
12. H. W. DINGES, B. KEMPF, H. BURKHARD and R. GOBEL, *ibid.* **50** (1991) 359.
13. P. G. SNYDER, M. C. ROST, G. H. BU-ABBUD, J. A. WOOLLAM and S. A. ALTEROVITZ, *J. Appl. Phys.* **60** (1986) 3293.

Received 3 November 1994
and accepted 21 February 1995